


 Cite this: *RSC Adv.*, 2025, **15**, 31154

# Cumingianols G and H, new 14,18-cycloapoeuphane triterpenoids from the Taiwan *Dysoxylum cumingianum* C. DC.†

 Thanh Hao Huynh,<sup>‡,ab</sup> Bo-Rong Peng,<sup>‡,ab</sup> Chi-Jen Tai,<sup>c</sup> Yu-Ting Hung,<sup>c</sup>  
 Yu-Chuan Su,<sup>c</sup> Jing-Lan Hu,<sup>c</sup> Jou-Hsuan Lee,<sup>c</sup> Chang-Yih Duh<sup>c</sup>  
 and Jing-Ru Weng<sup>\*,cde</sup>

Two new 14,18-cycloapoeuphane triterpenoids, cumingianols G (1) and H (2), along with 12 known compounds, cumingianol C (3), cumingianol A (4), cumingianol D (5), 3,3-ethylenedioxy-5 $\alpha$ -cycloart-24-en-23-one (6), 24,25(*R,S*)-24,25-epoxy-20(*S*)-hydroxydammar-3-one (7), (3 $\beta$ ,7 $\alpha$ )-stigmast-5-ene-3,7-diol (8), 7 $\alpha$ -hydroxystigmasterol (9), 7 $\beta$ -hydroxysitosterol (10), 7 $\beta$ -hydroxystigmasterol (11), ethylcholest-5-en-3-hydroxy-7-one (12), coniferaldehyde (13) and 4-hydroxy-3,5-dimethoxy-benzaldehyde (14), have been isolated from *Dysoxylum cumingianum* collected in Taiwan. The structures of these metabolites were determined through mass spectrometry and 1D and 2D NMR analyses, combined with comparisons to reference data. The cytotoxic effects of these isolates were evaluated against human oral squamous cell carcinoma (SCC2095), human breast adenocarcinoma (MCF-7), and human gastric adenocarcinoma (SCM-1). Among them, compound 4 exhibited significant cytotoxicity against the SCC2095 and MCF-7 cell lines, with IC<sub>50</sub> values of 6.3  $\mu$ M and 6.1  $\mu$ M, respectively.

 Received 27th May 2025  
 Accepted 22nd July 2025

DOI: 10.1039/d5ra03726c

[rsc.li/rsc-advances](http://rsc.li/rsc-advances)

## Introduction

Cancer remains one of the most lethal diseases worldwide. In 2022, nearly 20 million new cancer cases and 9.7 million cancer-related deaths were reported, according to the latest data from the International Agency for Research on Cancer.<sup>1</sup> Current estimates indicate that about one in five individuals will develop cancer during their lifetime, while approximately one in nine men and one in 12 women will die from it.<sup>1</sup> The most frequently diagnosed cancers globally included breast cancer in women, lung cancer, and prostate cancer, while the leading causes of cancer-related deaths were lung, liver, and stomach cancers.<sup>2</sup> In response to the growing global cancer burden, botanical herbs and their derived compounds are receiving

increasing attention as complementary sources for cancer therapy. Numerous clinical studies have demonstrated the beneficial effects of herbal medicines on patient survival, immune system modulation, and quality of life, particularly when used in combination with conventional treatments.<sup>3</sup>

Among the diverse plant species explored for their medicinal potential, the genus *Dysoxylum*, belonging to the Mahogany family (Meliaceae), has been traditionally used in Southeast Asia and India for treating various ailments.<sup>4,5</sup> These plants are known to contain structurally diverse compounds with a broad range of biological activities, including anticancer,<sup>6–8</sup> antibacterial,<sup>7</sup> anti-inflammatory,<sup>9,10</sup> and anti-leishmania properties.<sup>11</sup> Natural compounds derived from the genus *Dysoxylum* predominantly include sesquiterpenoids, diterpenoids, triterpenoids, triterpenoid glycosides, limonoids, steroids, and alkaloids.<sup>7,12</sup> Among these, triterpenoids and triterpenoid glycosides are the most abundant. These compounds exhibit a wide structural diversity, encompassing dammarane, ole-anane, lupane, tirucallane, cyclolanostane, cycloartane, glabretal, cycloapoeuphane, and nortriterpenoid types.<sup>7,12</sup> Among the species in the genus *Dysoxylum*, *D. cumingianum*, found in the Philippines, northern Borneo, and Taiwan,<sup>13,14</sup> is one such species of interest. In addition to their remarkable structural diversity, the secondary metabolites derived from *D. cumingianum* have demonstrated notable pharmaceutical potential, particularly exhibiting anti-cancer activity.<sup>8,15–19</sup> The stigmastane-type sterol dycusin A and the triterpenes cumingianols A, B, and D have demonstrated enhanced cytotoxicity

<sup>a</sup>Center for Drug Research and Development, College of Human Ecology, Chang Gung University of Science and Technology, Taoyuan 333324, Taiwan

<sup>b</sup>Graduate Institute of Health Industry Technology, College of Human Ecology, Chang Gung University of Science and Technology, Taoyuan 333324, Taiwan

<sup>c</sup>Department of Marine Biotechnology and Resources, National Sun Yat-sen University, Kaohsiung 804201, Taiwan. E-mail: [columnster@gmail.com](mailto:columnster@gmail.com)

<sup>d</sup>Graduate Institute of Natural Products, Kaohsiung Medical University, Kaohsiung 807378, Taiwan

<sup>e</sup>Graduate Institute of Pharmacognosy, College of Pharmacy, Taipei Medical University, Taipei 110301, Taiwan

† The authors have been unable to contact Chi-Jen Tai to confirm the final version and author list, however National Sun Yat-sen University has provided formal approval of the authorship.

‡ These authors have contributed equally to this work.



against multi-drug resistant KB-C2 cancer cells.<sup>15,16</sup> Notably, the triterpene glucoside cumingianoside P showed significant cytotoxic effects against 37 human cancer cell lines, and most sensitive to the renal cancer UO-31 cells which the  $EC_{50}$  value of 0.267  $\mu\text{M}$ , while the cumingianoside Q displayed selective cytotoxicity against non-small cell lung cancer NCI-H522 cells which the  $EC_{50}$  value of 1.67  $\mu\text{M}$ .<sup>18</sup> Additionally, cumingianoside M, a triterpene glucoside featuring a 14,18-cycloapoeuphane skeleton, showed significant cytotoxic activity against various cancer cells, especially leukemia and melanoma cell lines.<sup>17</sup> Furthermore, cumingianosides A and C also demonstrated strong selective cytotoxic effects against the human leukemia MOLT-4 cell line which the  $ED_{50}$  values of <0.00625 and <0.0045  $\mu\text{g mL}^{-1}$ , respectively.<sup>8</sup>

In an effort to identify antitumor compounds from plants native to Taiwan, we aimed to develop botanical drugs for cancer treatment. In this study, we discovered two new 14,18-cycloapoeuphane-type triterpenoids, cumingianols G (1) and H (2), along with 12 known compounds, including cumingianol C (3),<sup>15</sup> cumingianol A (4),<sup>15</sup> cumingianol D (5),<sup>15</sup> 3,3-ethylenedioxy-5 $\alpha$ -cycloart-24-en-23-one (6),<sup>20</sup> 24,25(*R,S*)-24,25-epoxy-20(*S*)-hydroxydammar-3-one (7),<sup>21</sup> (3 $\beta$ ,7 $\alpha$ )-stigmast-5-ene-3,7-diol (8),<sup>22</sup> 7 $\alpha$ -hydroxystigmast-5-ene-3-one (9),<sup>23</sup> 7 $\beta$ -hydroxystigmast-5-ene-3-one (10),<sup>24</sup> 7 $\beta$ -hydroxystigmast-5-ene-3-one (11),<sup>23</sup> ethylcholest-5-en-3-hydroxy-7-one (12),<sup>25</sup> coniferaldehyde (13),<sup>26</sup> and 4-hydroxy-3,5-dimethoxybenzaldehyde (14)<sup>27</sup> (Fig. 1). These compounds were isolated from the methanol and acetone extracts of the stems of *D. cumingianum* collected in Taiwan. The structures of

compounds 1–14 were elucidated through detailed analyses of their MS, IR, and NMR spectra. The cytotoxic activity of the isolated compounds was evaluated against three human cancer cell lines: oral squamous cell carcinoma (SCC2095), breast adenocarcinoma (MCF-7), and gastric adenocarcinoma (SCM-1). Among them, compound 4 exhibited significant cytotoxicity against the SCC2095 and MCF-7 cell lines, with  $IC_{50}$  values of 6.3  $\mu\text{M}$  and 6.1  $\mu\text{M}$ , respectively.

## Results and discussion

Compound 1 was isolated as an amorphous powder with the molecular formula  $C_{35}H_{58}O_6$  (seven degrees of unsaturation), established based on an ESIMS peak at  $m/z$  597, and further confirmed by a HRESIMS peak at  $m/z$  597.4125  $[M + Na]^+$  (calcd. for  $C_{35}H_{58}O_6Na$ , 597.4126). The IR spectrum of 1 indicated the presence of hydroxy and ester moieties, corresponding to absorption bands at  $\nu_{\text{max}}$  3477 and 1713  $\text{cm}^{-1}$ , respectively. The  $^{13}\text{C}$  NMR data of 1, in combination with DEPT spectrum, showed resonances of 35 carbons, including one ester carbonyl ( $\delta_{\text{C}}$  170.4, OAc-7), one ketal carbon ( $\delta_{\text{C}}$  108.4, acetonide ketal carbon), five  $\text{sp}^3$  oxygenated carbons ( $\delta_{\text{C}}$  87.8, C-24; 77.6, C-23; 76.3, C-7; 76.0, C-3; 69.8, C-5), five  $\text{sp}^3$  quaternary carbons, four  $\text{sp}^3$  methine carbons, nine  $\text{sp}^3$  methylene carbons, and ten methyl carbons (Table 1). The  $^1\text{H}$  NMR data of 1, in combination with the HSQC spectrum, revealed the presence of a cyclopropyl methylene group ( $\delta_{\text{H}}$  0.37, 1H, d,  $J = 5.4$  Hz and 0.66, 1H, d,  $J = 5.4$  Hz/ $\delta_{\text{C}}$  16.2,  $\text{CH}_2$ -18), four  $\text{sp}^3$  oxygenated methine

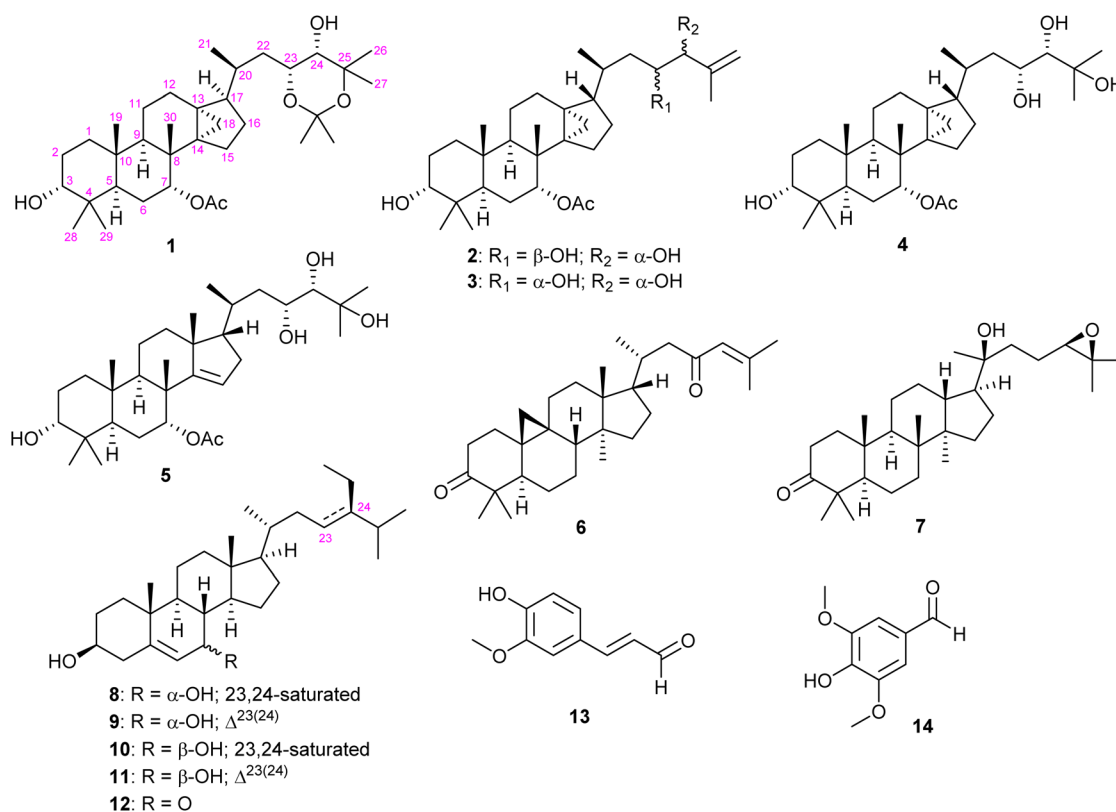


Fig. 1 The structures of compounds 1–14.



Table 1  $^1\text{H}$  (600 MHz,  $\text{CDCl}_3$ ) and  $^{13}\text{C}$  (150 MHz,  $\text{CDCl}_3$ ) NMR data for **1**

Position	$\delta_{\text{H}}$ ( $J$ in Hz)	$\delta_{\text{C}}$ , Mult. <sup>a</sup>
1	1.30 m; 1.38 m	33.3, CH <sub>2</sub>
2	1.56 m; 1.95 m	25.1, CH <sub>2</sub>
3	3.41 t (2.4)	76.0, CH
4		37.0, C
5	1.81 m	41.2, CH
6	1.54 m; 1.63 m	23.3, CH <sub>2</sub>
7	4.93 dd (3.6, 1.8)	76.3, CH
8		34.8, C
9	1.32 m	45.5, CH
10		37.2, C
11	1.27 m	16.8, CH <sub>2</sub>
12	1.68 m; 1.83 m	27.6, CH <sub>2</sub>
13		27.6, C
14		38.2, C
15	1.33 m; 1.75 m	26.4, CH <sub>2</sub>
16	0.80 m; 1.50 m	24.4, CH <sub>2</sub>
17	1.80 m	52.2, CH
18	0.37 d (5.4); 0.66 d (5.4)	16.2, CH <sub>2</sub>
19	0.89 s	15.9, CH <sub>3</sub>
20	1.74 m	34.6, CH
21	1.02 d (7.2)	20.1, CH <sub>3</sub>
22	1.28 m; 1.81 m	38.8, CH <sub>2</sub>
23	3.94 ddd (9.0, 7.2, 2.4)	77.6, CH
24	3.48 d (7.2)	87.8, CH
25		69.8, C
26	1.16 s	24.6, CH <sub>3</sub>
27	1.25 s	28.0, CH <sub>3</sub>
28	0.85 s	28.0, CH <sub>3</sub>
29	0.81 s	21.9, CH <sub>3</sub>
30	1.08 s	19.6, CH <sub>3</sub>
OAc-7	2.03 s	21.6, CH <sub>3</sub> 170.4, C
Acetone	1.39 s	27.2, CH <sub>3</sub>
	1.38 s	27.5, CH <sub>3</sub> 108.4, C

<sup>a</sup> Multiplicity deduced by DEPT and HSQC spectra.

groups ( $\delta_{\text{H}}$  4.93, 1H, t,  $J = 2.4$  Hz/ $\delta_{\text{C}}$  76.3, CH-7;  $\delta_{\text{H}}$  3.94, 1H, ddd,  $J = 9.0, 7.2, 2.4$  Hz/ $\delta_{\text{C}}$  77.6, CH-23;  $\delta_{\text{H}}$  3.48, 1H, d,  $J = 7.2$  Hz/ $\delta_{\text{C}}$  87.8, CH-24;  $\delta_{\text{H}}$  3.41, 1H, t,  $J = 2.4$  Hz/ $\delta_{\text{C}}$  76.0, CH-3), one acetoxy substituent ( $\delta_{\text{H}}$  2.03, 3H, s/ $\delta_{\text{C}}$  21.6, acetate methyl;  $\delta_{\text{C}}$  170.4, acetate carbonyl), one doublet methyl, and eight singlet methyls (Table 1). These data indicated that the structure of **1** is consistent with a 14,18-cyclopotirucallane-type triterpenoid.<sup>15</sup> Interpretation of  $^1\text{H}$ - $^1\text{H}$  correlations observed in the COSY spectra enabled the establishment of four continuous spin systems H<sub>2</sub>-1/H<sub>2</sub>-2/H-3, H-5/H<sub>2</sub>-6/H-7, H-9/H<sub>2</sub>-11/H<sub>2</sub>-12, H<sub>2</sub>-15/H<sub>2</sub>-16/H-17/H-20/H<sub>2</sub>-22/H-23/H-24, and H-20/H<sub>3</sub>-21 (Fig. 2). Correlations between protons and non-protonated carbons were observed in the HBMBC spectrum, such as H-3, H-5, H<sub>3</sub>-28, H<sub>3</sub>-29/C-4; H-7, H-9, H<sub>2</sub>-18, H<sub>3</sub>-30/C-8; H<sub>2</sub>-1, H-5, H-9, H<sub>3</sub>-19/C-10; H<sub>2</sub>-12, H-17, H<sub>2</sub>-18/C-13; H-7, H<sub>2</sub>-15, H<sub>2</sub>-18, H<sub>3</sub>-30/C-14; and H-23, H-24, H<sub>3</sub>-26, H<sub>3</sub>-27/C-25 (Fig. 2). These COSY and HBMBC analyses confirmed the 14,18-cyclopotirucallane-type triterpenoid skeleton of **1**. The position of the acetoxy substituent at C-7 was confirmed by the HBMBC correlation from H-7 ( $\delta_{\text{H}}$  4.93) to the acetoxy carbonyl at  $\delta_{\text{C}}$  170.4 (Fig. 2). The

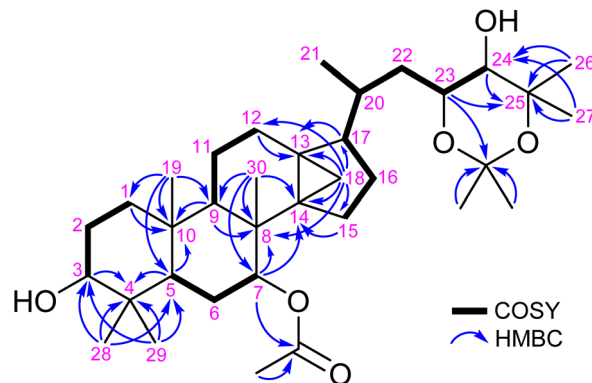


Fig. 2 Key COSY and HMBC correlations of **1**.

acetonide moiety was indicated by the presence of a ketal carbon ( $\delta_{\text{H}}$  108.4, C) and two singlet methyls ( $\delta_{\text{H}}$  1.39, 3H, s/ $\delta_{\text{C}}$  27.2, CH<sub>3</sub>;  $\delta_{\text{H}}$  1.38, 3H, s/ $\delta_{\text{C}}$  27.5, CH<sub>3</sub>),<sup>29</sup> both of which showed correlation with the ketal carbon in the HMBC spectrum. This finding was consistent with the seven degrees of unsaturation in **1**. In the HMBC spectrum, H-23 ( $\delta_{\text{H}}$  3.94) showed a correlation with the acetonide ketal carbon, while H-24 ( $\delta_{\text{H}}$  3.48) did not. Therefore, the acetonide moiety should be positioned between C-23 and C-25 ( $\delta_{\text{C}}$  69.8, oxygenated tertiary carbon) forming a six-membered acetonide moiety (Fig. 2). Based on the chemical shifts of CH-3 ( $\delta_{\text{H}}$  3.41/ $\delta_{\text{C}}$  76.0) and CH-24 ( $\delta_{\text{H}}$  3.48/ $\delta_{\text{C}}$  87.8), the remaining two hydroxy groups are placed at C-3 and C-24. The planar structure of **1** was thus fully established.

The relative stereochemistry of **1** was established by interpreting the NOESY correlations in combination with a computer-generated structural model. In the NOESY spectrum (Fig. 3), H<sub>3</sub>-19 showed correlations with H<sub>3</sub>-29 and H<sub>3</sub>-30, while H-5 correlated with H-9 and H<sub>3</sub>-28, indicating that the Me-19 and Me-30 are  $\beta$ -oriented, and H-5 and H-9 are  $\alpha$ -oriented. H-3 exhibited NOE correlations with both protons of CH<sub>2</sub>-2 ( $\delta_{\text{H}}$  1.56 and 1.95) as well as with H<sub>3</sub>-28 and H<sub>3</sub>-29. H-7 exhibited NOE correlations with H<sub>3</sub>-30 and both protons of CH<sub>2</sub>-6 ( $\delta_{\text{H}}$  1.54 and 1.63). Based on the structural model, H-3 and H-7 are oriented to the  $\alpha$ -face, while OH-3 and OAc-7 are oriented to the  $\beta$ -face. One proton of CH<sub>2</sub>-18 ( $\delta_{\text{H}}$  0.66) correlated with H-9, and

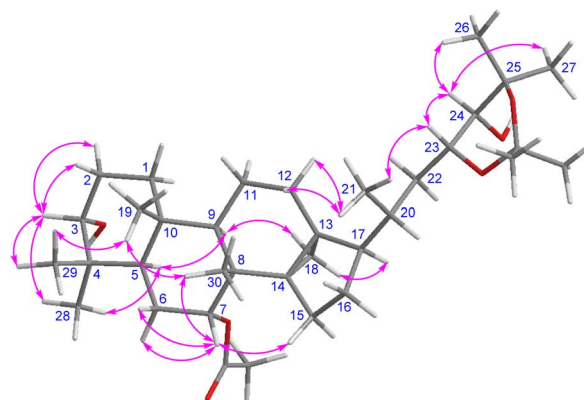


Fig. 3 Key NOESY correlations of **1**.



the other proton ( $\delta_{\text{H}}$  0.37) correlated with H-17 ( $\delta_{\text{H}}$  1.80), suggesting that CH<sub>2</sub>-18 and H-17 are  $\alpha$ -oriented, the same as H-9. H<sub>3</sub>-21 showed NOE correlations with both protons of H<sub>2</sub>-12 ( $\delta_{\text{H}}$  1.68 and 1.83) and with H-23. Considering the model structure, H<sub>3</sub>-21 should be positioned in the  $\beta$ -orientation at C-20. H-23 correlated with H<sub>3</sub>-21, while H-24 correlated with H-23 as well as H<sub>3</sub>-26 and H<sub>3</sub>-27. Additionally, H-23 coupled with H-24 with a <sup>3</sup>*J* coupling constant of *J* = 7.2 Hz, based on the Karplus equation,<sup>30</sup> the dihedral angle between H-23 and H-24 was approximately 50°. In combination with the structural model, these two protons are oriented in the  $\beta$ -orientation. Therefore, the relative stereochemistry of **1** was established as 3*R*\*,5*R*\*,7*R*\*,8*R*\*,9*R*\*,10*S*\*,13*R*\*,14*S*\*,17*R*\*,20*S*\*,23*R*\*,24*S*\*. To determine whether isolate **1** was a natural or an artifactual compound, the original MeOH extract was re-examined by LC-MS. The LC-MS profile showed that the MeOH extract contained **1**, which indicated by a pseudo-molecular ion peak at *m/z* 575 [M + 1]<sup>+</sup> (Fig. S57). The isolate **1** was thus identified as a new compound and named cumingianol G.

Compound **2** was obtained as an amorphous powder. Its HRESIMS spectrum showed an ion peak at *m/z* 539.3709 [M + Na]<sup>+</sup> (calcd. for C<sub>32</sub>H<sub>52</sub>O<sub>5</sub>Na, 539.3707), indicating a molecular

formula C<sub>32</sub>H<sub>52</sub>O<sub>5</sub> (seven degrees of unsaturation). The presence of hydroxy, ester carbonyl, and olefinic functional groups was confirmed by IR absorption bands at  $\nu_{\text{max}}$  3518, 1731, and 1652 cm<sup>-1</sup>, respectively. Analysis of <sup>1</sup>H, <sup>13</sup>C, DEPT, and HSQC NMR data of **2**, revealed the presence of an acetoxy substituent, an exocyclic olefin, a cyclopropyl methylene moiety, four oxygenated methines, one doublet methyl, and five other singlet methyls (Table 2). The planar structure of **2**, including the positions of OAc-7, OH-3, OH-23, and OH-24, was fully determined by interpreting the correlations observed in the COSY and HMBC spectra (Fig. 4). It was found that the planar structure of **2** is identical to that of cumingianol C (**3**). However, comparison of the NMR data between **2** and cumingianol C (**3**) revealed marked differences in their <sup>1</sup>H and <sup>13</sup>C chemical shifts (Table 2). A closer analysis of the NMR data for CH-23 ( $\delta_{\text{H}}$  3.85, dd, *J* = 13.6, 8.0 Hz;  $\delta_{\text{C}}$  78.1), CH-24 ( $\delta_{\text{H}}$  3.95, d, *J* = 8.0 Hz;  $\delta_{\text{C}}$  86.4), C-25 ( $\delta_{\text{C}}$  142.1), CH<sub>2</sub>-26 ( $\delta_{\text{H}}$  4.98, br s; 5.05 br s/ $\delta_{\text{C}}$  115.2), and CH<sub>3</sub>-27 ( $\delta_{\text{H}}$  1.79, s;  $\delta_{\text{C}}$  17.5) of **2** with those of **3** ( $\delta_{\text{H}}$  3.71, dd, *J* = 12.0, 4.8 Hz/ $\delta_{\text{C}}$  71.3, CH-23;  $\delta_{\text{H}}$  3.87, d, *J* = 4.8 Hz/ $\delta_{\text{C}}$  77.8, CH-24;  $\delta_{\text{C}}$  145.0, C-25;  $\delta_{\text{H}}$  4.99 br s, 5.05 br s/ $\delta_{\text{C}}$  113.0, CH<sub>2</sub>-26;  $\delta_{\text{H}}$  1.76, s/ $\delta_{\text{C}}$  18.7, CH<sub>3</sub>-27), suggested differences in the configurations at positions CH-23 and CH-24. Further analysis of

Table 2 <sup>1</sup>H (400 MHz, CDCl<sub>3</sub>) and <sup>13</sup>C (100 MHz, CDCl<sub>3</sub>) NMR data for **2** and <sup>1</sup>H (600 MHz, CDCl<sub>3</sub>) and <sup>13</sup>C (150 MHz, CDCl<sub>3</sub>) NMR data for **3**

Position	<b>2</b>		<b>3</b>	
	$\delta_{\text{H}}$ ( <i>J</i> in Hz)	$\delta_{\text{C}}$ , Mult. <sup>a</sup>	$\delta_{\text{H}}$ ( <i>J</i> in Hz)	$\delta_{\text{C}}$ , Mult. <sup>a</sup>
1	1.32 m; 1.40 m	33.4, CH <sub>2</sub>	1.29 m; 1.38 m	33.2, CH <sub>2</sub>
2	1.56 m; 1.96 m	25.3, CH <sub>2</sub>	1.56 m; 1.95 m	25.1, CH <sub>2</sub>
3	3.42 br s	76.2, CH	3.41 t (3.0)	76.0, CH
4		37.2, C		37.0, C
5	1.84 m	41.3, CH	1.82 m	41.2, CH
6	1.56 m; 1.62 m	23.5, CH <sub>2</sub>	1.54 m; 1.64 m	23.3, CH <sub>2</sub>
7	5.00 br s	76.5, CH	4.98 br s	76.3, CH
8		38.3, C		38.2, C
9	1.33 m	45.7, CH	1.33 m	45.5, CH
10		37.4, C		37.2, C
11	1.28 m	17.0, CH <sub>2</sub>	1.27 m	16.8, CH <sub>2</sub>
12	1.69 m; 1.81 m	27.7, CH <sub>2</sub>	1.70 m; 1.82 m	27.6, CH <sub>2</sub>
13		27.6, C		27.5, C
14		35.0, C		34.9, C
15	1.34 m; 1.75 m	26.6, CH <sub>2</sub>	1.34 m; 1.76 m	26.4, CH <sub>2</sub>
16	0.81 m; 1.48 m	24.1, CH <sub>2</sub>	0.84 m; 1.50 m	24.4, CH <sub>2</sub>
17	1.78 m	52.5, CH	1.81 m	52.3, CH
18	0.37 d (4.8); 0.65 d (4.8)	16.5, CH <sub>2</sub>	0.38 d (5.4); 0.66 d (5.4)	16.2, CH <sub>2</sub>
19	0.89 s	16.1, CH <sub>3</sub>	0.89 s	15.9, CH <sub>3</sub>
20	1.70 m	33.0, CH	1.71 m	32.8, CH
21	0.95 d (6.4)	20.1, CH <sub>3</sub>	0.99 d (6.6)	19.9, CH <sub>3</sub>
22	1.35 m; 1.72 m	36.2, CH <sub>2</sub>	1.19 m; 1.76 m	36.5, CH <sub>2</sub>
23	3.85 dd (13.6, 8.0)	78.1, CH	3.71 dd (12.0, 4.8)	71.3, CH
24	3.95 d (8.0)	86.4, CH	3.87 d (4.8)	77.8, CH
25		142.1, C		145.0, C
26	4.98 br s; 5.05 br s	115.2, CH <sub>2</sub>	4.99 br s; 5.05 br s	113.0, CH <sub>2</sub>
27	1.79 s	17.5, CH <sub>3</sub>	1.76 s	18.7, CH <sub>3</sub>
28	0.85 s	28.2, CH <sub>3</sub>	0.85 s	28.0, CH <sub>3</sub>
29	0.81 s	22.1, CH <sub>3</sub>	0.81 s	21.9, CH <sub>3</sub>
30	1.08 s	19.8, CH <sub>3</sub>	1.08 s	19.6, CH <sub>3</sub>
OAc-7	2.04 s	21.8, CH <sub>3</sub>	2.03 s	21.6, C
		170.6, C		170.4, C

<sup>a</sup> Multiplicity deduced by DEPT and HSQC spectra.



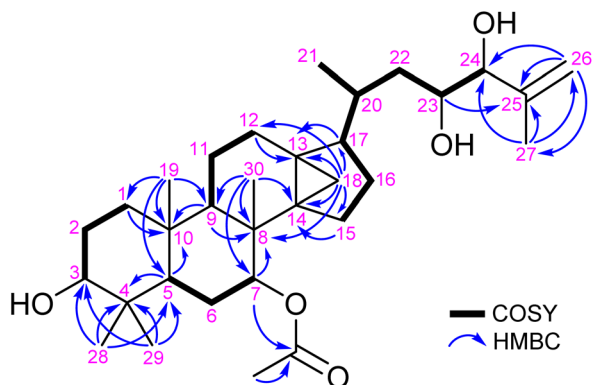


Fig. 4 Key COSY and HMBC correlations of **2**.

correlations observed in the NOESY spectrum (Fig. 5), revealed that H-3 showed correlations with both protons of CH<sub>2</sub>-2 and with H<sub>3</sub>-28 and H<sub>3</sub>-29; H-7 exhibited correlations with H<sub>3</sub>-30 and both protons of CH<sub>2</sub>-6, indicating that the hydroxyl at C-3 and the acetoxy group at C-7 are  $\alpha$ -positioned. Additionally, H-17 correlated with H<sub>3</sub>-30 and H<sub>3</sub>-21, suggesting that H-17 and CH<sub>3</sub>-21 are  $\beta$ -oriented, consistent with the orientation of CH<sub>3</sub>-30. A literature review indicated that *J* value for *cis* protons are approximately 6.0 Hz, while those for *trans* protons fall within the range of 7.3 to 8.4 Hz.<sup>31–34</sup> The *J*<sub>23,24</sub> of **2** was 8.0 Hz, which is more consistent with a *trans* configuration, whereas the corresponding value in **3** (*J*<sub>23,24</sub> = 4.8 Hz) supports a *cis* configuration. Furthermore, H-23 showed correlations with H-20, H<sub>3</sub>-21, and H<sub>3</sub>-27; H-24 correlated with one of the H<sub>2</sub>-22 protons ( $\delta_{\text{H}}$  1.72) and with H<sub>2</sub>-26. Considering the structural model, OH-23 and OH-24 are positioned on the  $\beta$ - and  $\alpha$ -faces, respectively, instead of  $\alpha$ - and  $\alpha$ -faces as those of cumingianol C (**3**). Thus, the relative stereochemistry of **2** was established as 3*R*\*,5*R*\*,7*R*\*,8*R*\*,9*R*\*,10*S*\*,13*R*\*,14*S*\*,17*S*\*,20*S*\*,23*S*\*,24*R*\*. Compound **2** was therefore identified as a new compound and named cumingianol H.

The known compounds **3–14** were identified as cumingianol C (**3**),<sup>15</sup> cumingianol A (**4**),<sup>15</sup> cumingianol D (**5**),<sup>15</sup> 3,3-ethylene-dioxy-5 $\alpha$ -cycloart-24-en-23-one (**6**),<sup>20</sup> 24,25(*R,S*)-24,25-epoxy-20(*S*)-hydroxydammar-3-one (**7**),<sup>21</sup> (3 $\beta$ ,7 $\alpha$ )-stigmast-5-ene-3,7-

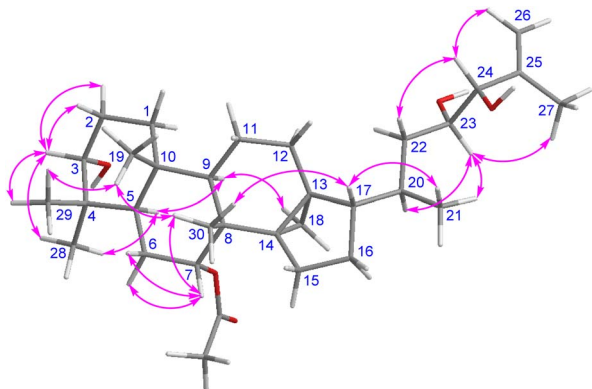


Fig. 5 Key NOESY correlations of **2**.

Table 3 Cytotoxicity of the compounds **1–14** against cancer cell lines

Compound	IC <sub>50</sub> ( $\mu\text{M}$ )			
	SCC2095 <sup>a</sup>	MCF-7 <sup>a</sup>	SCM-1 <sup>a</sup>	Fibroblasts
<b>1</b>	9.6 $\pm$ 0.6 <sup>b</sup>	7.6 $\pm$ 1.6	11.7 $\pm$ 1.5	18.4 $\pm$ 1.1
<b>2</b>	>10	>10	>10	—
<b>3</b>	>10	>10	>10	—
<b>4</b>	6.3 $\pm$ 1.0	6.1 $\pm$ 0.9	20.0 $\pm$ 4.9	>30
<b>5</b>	18.3 $\pm$ 1.9	13.3 $\pm$ 1.8	15.6 $\pm$ 3.6	>30
<b>6</b>	>30	>30	>30	—
<b>7</b>	>30	>30	>30	—
<b>8</b>	>30	>30	>30	—
<b>9</b>	>30	>30	>30	—
<b>10</b>	>30	>30	>30	—
<b>11</b>	23.9 $\pm$ 1.4	>30	>30	—
<b>12</b>	>30	>30	>30	—
<b>13</b>	>30	>30	>30	—
<b>14</b>	>10	>10	>10	—
Etoposide	2.5 $\pm$ 0.2	—	—	—
Tamoxifen	—	7.0 $\pm$ 0.6	—	—
Paclitaxel	—	—	0.07 $\pm$ 0.002	—

<sup>a</sup> SCC2095: human oral squamous cell carcinoma; MCF-7: human breast adenocarcinoma; SCM-1: human gastric adenocarcinoma, fibroblasts. <sup>b</sup> Data are presented as mean  $\pm$  S.E.M. (*n* = 3). Tamoxifen or etoposide or paclitaxel was used as a positive control.

diol (**8**),<sup>22</sup> 7 $\alpha$ -hydroxystigmasterol (**9**),<sup>23</sup> 7 $\beta$ -hydroxysitosterol (**10**),<sup>24</sup> 7 $\beta$ -hydroxystigmasterol (**11**),<sup>23</sup> ethylcholest-5-en-3-hydroxy-7-one (**12**),<sup>25</sup> coniferaldehyde (**13**),<sup>26</sup> and 4-hydroxy-3,5-dimethoxybenzaldehyde (**14**),<sup>27</sup> respectively, by comparing their spectroscopic data with those data reported in previous publications.

The cytotoxicity of isolates **1–14** against SCC2095, MCF-7, and SCM-1 cancer cell lines was evaluated using the MTT assay. The results showed that compounds **1**, **4**, **5**, and **11** inhibited the proliferation of SCC2095, MCF-7, and SCM-1 cell lines (Table 3). Notably, compound **4** exhibited significant cytotoxicity against the SCC2095 and MCF-7 cell lines with IC<sub>50</sub> values of 6.3  $\pm$  1.0 and 6.1  $\pm$  0.9  $\mu\text{M}$ , respectively. To verify the selectivity of these compounds toward cancer cells, compounds **1**, **4**, and **5** were evaluated for their cytotoxicity against fibroblast cells. The results showed that compound **1** exhibited mild cytotoxicity, with an IC<sub>50</sub> value of 18.4  $\mu\text{M}$ , while compounds **4** and **5** were non-cytotoxic to this cell line (Table 3), supporting their selective cytotoxicity toward cancer cells. Compound **4** has also been reported to be cytotoxic to human epidermoid carcinoma KB and colchicine resistant KB-C2 cell lines.<sup>15</sup> Compounds **4** and **5** share the same number, type, and position of functional groups. The only structural difference is that compound **4** features a 14,18-cycloapoeuphanyl structure at the C-14 position, whereas compound **5** contains a 14,15 double bond. This 14,18-cycloapoeuphanyl structure in compound **4** may account for its enhanced cytotoxic activity against cancer cells.

## Conclusions

Two new 14,18-cycloapotirucallane-type triterpenoids, cumingianols G (**1**) and H (**2**), along with 12 known compounds,



including cumingianol C (3), cumingianol A (4), cumingianol D (5), 3,3-ethylenedioxy-5 $\alpha$ -cycloart-24-en-23-one (6), 24,25(*R,S*)-24,25-epoxy-20(*S*)-hydroxydammar-3-one (7), (3 $\beta$ ,7 $\alpha$ )-stigmast-5-ene-3,7-diol (8), 7 $\alpha$ -hydroxystigmasterol (9), 7 $\beta$ -hydroxystigmasterol (10), 7 $\beta$ -hydroxystigmasterol (11), ethylcholest-5-en-3-hydroxy-7-one (12), coniferaldehyde (13) and 4-hydroxy-3,5-dimethoxybenzaldehyde (14), were isolated and characterized from the Taiwan *D. cumingianum*. Among these secondary metabolites, compound 4 demonstrated superior biological activity in inhibiting the growth of these three cancer cell lines, possibly due to its 14,18-cycloapoephanyl structure. This finding aligns with previous literature reports, indicating that compound 4 holds potential for anti-cancer medical applications.

## Experimental

### General procedures

NMR spectra were recorded using a Varian VNMRS-400 or a JEOL ECZ-600R NMR spectrometers. Optical rotation measurements were performed with a Jasco P-2000 polarimeter. IR spectra were obtained using a Jasco FTIR-4X spectrophotometer. ESI-MS and HR-ESI-MS analyses were conducted on a Bruker APEX-II mass spectrometer. Column chromatography was carried out using silica gel (40–63  $\mu$ m, Merck) and spherical C18 100 Å reversed-phase silica gel (40–63  $\mu$ m, LiChroprep). Thin-layer chromatography (TLC) was performed on silica gel 60 F<sub>254</sub> plates (100  $\mu$ m, Merck). Medium-pressure liquid chromatography (MPLC) was conducted using an EYELA ceramic pump VSP-3050. Reverse-phase HPLC (RP-HPLC) was performed using a Hitachi L-5430 HPLC detector and a Hitachi model L-5110 pump, equipped with a Supelco RP column (250  $\times$  10 mm, 5  $\mu$ m).

### Plant material

The whole plant of *D. cumingianum* was collected in July 2016 from Taitung County, Taiwan. The scientific identification of the specimen was confirmed by Dr Chang-Yih Duh, and a voucher specimen (2016) was deposited in the Department of Marine Biotechnology and Resources, National Sun Yat-sen University, Kaohsiung, Taiwan.

### Extraction and isolation

The stems of *D. cumingianum* (dry weight 8.6 kg) were extracted at room temperature with methanol (MeOH, 40 L  $\times$  3) and acetone (40 L  $\times$  3), yielding the Dc-MeOH extract (89.8 g) and Dc-Acetone extract (77.3 g), respectively. The Dc-MeOH extract was partitioned between ethyl acetate (EtOAc) and H<sub>2</sub>O to yield the Dc-MeOH-EtOAc layer (25.2 g), which was further partitioned between MeOH and *n*-hexane to obtain the MeOH layer Dc-M (19.0 g). Dc-M was subjected to silica gel column chromatography using a stepwise gradient of *n*-hexane/acetone (100% to 0%) followed by acetone/MeOH (100% to 0%), affording seven fractions (Dc-M-A to Dc-M-G). Dc-M-B (4.62 g) was chromatographed on a silica gel column with *n*-hexane/EtOAc (1 : 1) to yield eight fractions (Dc-M-B-1 to Dc-M-B-8).

Dc-M-B-4 (410.0 mg) was further chromatographed using dichloromethane (DCM)/EtOAc (9 : 1) to yield nine subfractions (Dc-M-B-4-1 to Dc-M-B-4-9). Dc-M-B-4-6 (19.0 mg) was purified by silica gel MPLC using *n*-hexane/EtOAc (7 : 1) to obtain compound 2 (7.8 mg). Dc-M-B-7 was chromatographed on silica gel using chloroform/MeOH (8 : 1) to give five subfractions (Dc-M-B-7-1 to Dc-M-B-7-5). Dc-M-B-7-3 was purified by silica gel MPLC with *n*-hexane/acetone (1 : 1), followed by RP-HPLC with acetonitrile (ACN)/H<sub>2</sub>O (75%), yielding compound 1 (18.5 mg).

The Dc-Acetone extract was partitioned between EtOAc and water to yield the EtOAc-soluble layer (Dc-A, 64.1 g). This was subjected to silica gel column chromatography using a gradient of *n*-hexane/acetone (0% to 100%) followed by acetone/MeOH (0% to 100%), affording seven fractions (Dc-A-1 to Dc-A-7). Dc-A-2 (3.75 g) was chromatographed on silica gel using *n*-hexane/EtOAc (7 : 1) to produce eight subfractions (Dc-A-2-1 to Dc-A-2-8). Dc-A-2-4 (530 mg) was chromatographed with *n*-hexane/EtOAc (9 : 1), yielding three subfractions (Dc-A-2-4-1 to Dc-A-2-4-3). Dc-A-2-4-2 (10.3 mg) was purified *via* silica gel MPLC using *n*-hexane/EtOAc (1 : 1) to afford compound 6 (7.8 mg). Dc-A-2-7 (832.6 mg) was separated by silica gel chromatography with *n*-hexane/acetone (4 : 1) to give seven subfractions (Dc-A-2-7-1 to Dc-A-2-7-7). Dc-A-2-7-5 (77.0 mg) was purified by silica gel MPLC using *n*-hexane/EtOAc (3 : 1) to give six subfractions (Dc-A-2-7-5-1 to Dc-A-2-7-5-6). Dc-A-2-7-5-2 (4.7 mg) was further purified with *n*-hexane/acetone (4 : 1) to yield compound 12 (2.9 mg). Dc-A-2-7-5-4 (6.1 mg) was purified by RP-HPLC with MeOH/H<sub>2</sub>O (24 : 1) to obtain compounds 10 (2.6 mg) and 11 (0.9 mg). Dc-A-2-7-5-5 (6.2 mg) was purified using RP-HPLC with MeOH/H<sub>2</sub>O (24 : 1) to yield compounds 8 (3.3 mg) and 9 (1.0 mg). Dc-A-3 (7.0 g) was chromatographed over silica gel using a stepwise gradient of *n*-hexane/acetone (0% to 100%) to give four fractions (Dc-A-3-1 to Dc-A-3-4). Dc-A-3-2 (1.3 g) was re-chromatographed with *n*-hexane/DCM (1 : 1) to yield four subfractions (Dc-A-3-2-1 to Dc-A-3-2-4). Dc-A-3-2-4 (300.0 mg) was further purified on a silica gel column with *n*-hexane/EtOAc (4 : 1) to obtain four subfractions (Dc-A-3-2-4-1 to Dc-A-3-2-4-4). Dc-A-3-2-4-2 (27.5 mg) was purified using silica gel MPLC with *n*-hexane/acetone (14 : 1), followed by RP-HPLC with MeOH/H<sub>2</sub>O (19 : 1), to yield compound 7 (15.9 mg). Dc-A-6 (1.6 g) was chromatographed over silica gel with *n*-hexane/acetone (2 : 1) to produce four fractions (Dc-A-6-1 to Dc-A-6-4). Dc-A-6-2 (748.5 mg) was re-chromatographed using *n*-hexane/EtOAc (6 : 1) to give four subfractions (Dc-A-6-2-1 to Dc-A-6-2-4). Dc-A-6-2-1 (283.4 mg) was isolated using DCM/acetone (9 : 1), producing five subfractions (Dc-A-6-2-1-1 to Dc-A-6-2-1-5). Dc-A-6-2-1-2 (55.1 mg) was purified using reversed-phase open column chromatography with MeOH/H<sub>2</sub>O (7 : 3), followed by RP-HPLC with ACN/H<sub>2</sub>O (2 : 3), yielding compounds 13 (30.0 mg) and 14 (7.4 mg). Dc-A-6-2-1-5 (72.6 mg) was purified by RP-HPLC with MeOH/H<sub>2</sub>O (83 : 17) to obtain compound 3 (63.8 mg). Finally, Dc-A-6-2-4 (383.7 mg) was subjected to reversed-phase open column chromatography with MeOH/H<sub>2</sub>O (92 : 8) to yield six subfractions (Dc-A-6-2-4-1 to Dc-A-6-2-4-6). Dc-A-6-2-4-2 (40.3 mg) was purified using silica gel MPLC with *n*-hexane/acetone (5 : 1), followed by RP-HPLC with ACN/H<sub>2</sub>O (3 : 1), to yield compound 5 (27.0 mg). Dc-A-6-2-4-6 (149.3 mg) was purified by



silica gel MPLC with *n*-hexane/acetone (4 : 1), followed by RP-HPLC with ACN/H<sub>2</sub>O (7 : 3), affording compound **4** (100.0 mg).

**Cumingianol G (1).** Amorphous powder;  $[\alpha]_{\text{D}}^{22} = -18$  (*c* 0.02, CHCl<sub>3</sub>); IR (neat)  $\nu_{\text{max}}$  3477 and 1713 cm<sup>-1</sup>; <sup>1</sup>H (600 MHz, CDCl<sub>3</sub>) and <sup>13</sup>C (150 MHz, CDCl<sub>3</sub>) NMR data, see Table 1; ESIMS *m/z* 597 [M + Na]<sup>+</sup>; HRESIMS *m/z* 597.4125 [M + Na]<sup>+</sup> (calcd. for C<sub>35</sub>H<sub>58</sub>O<sub>6</sub>Na, 597.4126).

**Cumingianol H (2).** Amorphous powder;  $[\alpha]_{\text{D}}^{22} = -48$  (*c* 0.47, CHCl<sub>3</sub>); IR (neat)  $\nu_{\text{max}}$  3518, 1731, and 1652 cm<sup>-1</sup>; <sup>1</sup>H (400 MHz, CDCl<sub>3</sub>) and <sup>13</sup>C (100 MHz, CDCl<sub>3</sub>) NMR data, see Table 2; ESIMS *m/z* 539 [M + Na]<sup>+</sup>; HRESIMS *m/z* 539.3709 [M + Na]<sup>+</sup> (calcd. for C<sub>32</sub>H<sub>52</sub>O<sub>5</sub>Na, 539.3707).

**Cumingianol C (3).** Amorphous powder; <sup>1</sup>H and <sup>13</sup>C NMR data (Fig. S21–S23) were found to be in agreement with previous study;<sup>15</sup> ESIMS *m/z* 539 [M + Na]<sup>+</sup>.

**Cumingianol A (4).** Amorphous powder; <sup>1</sup>H and <sup>13</sup>C NMR data (Fig. S24–S26) were found to be in agreement with previous study;<sup>15</sup> ESIMS *m/z* 557 [M + Na]<sup>+</sup>.

**Cumingianol D (5).** Amorphous powder; <sup>1</sup>H and <sup>13</sup>C NMR data (Fig. S27–S29) were found to be in agreement with previous study;<sup>15</sup> ESIMS *m/z* 557 [M + Na]<sup>+</sup>.

**3,3-Ethylenedioxy-5 $\alpha$ -cycloart-24-en-23-one (6).** Amorphous powder; <sup>1</sup>H and <sup>13</sup>C NMR data (Fig. S30–S32) were found to be in agreement with previous study;<sup>20</sup> ESIMS *m/z* 439 [M + H]<sup>+</sup>.

**24,25(R,S)-24,25-Epoxy-20(S)-hydroxydammar-3-one (7).** Amorphous powder; <sup>1</sup>H and <sup>13</sup>C NMR data (Fig. S33–S35) were found to be in agreement with previous study;<sup>21</sup> ESIMS *m/z* 481 [M + Na]<sup>+</sup>.

**(3 $\beta$ ,7 $\alpha$ )-Stigmast-5-ene-3,7-diol (8).** Amorphous powder; <sup>1</sup>H and <sup>13</sup>C NMR data (Fig. S36–S38) were found to be in agreement with previous study;<sup>22</sup> ESIMS *m/z* 453 [M + Na]<sup>+</sup>.

**7 $\alpha$ -Hydroxystigmasterol (9).** Amorphous powder; <sup>1</sup>H and <sup>13</sup>C NMR data (Fig. S39–S41) were found to be in agreement with previous study;<sup>23</sup> ESIMS *m/z* 451 [M + Na]<sup>+</sup>.

**7 $\beta$ -Hydroxysitosterol (10).** Amorphous powder; <sup>1</sup>H and <sup>13</sup>C NMR data (Fig. S42–S44) were found to be in agreement with previous study;<sup>24</sup> ESIMS *m/z* 453 [M + Na]<sup>+</sup>.

**7 $\beta$ -Hydroxystigmasterol (11).** Amorphous powder; <sup>1</sup>H and <sup>13</sup>C NMR data (Fig. S45–S47) were found to be in agreement with previous study;<sup>23</sup> ESIMS *m/z* 451 [M + Na]<sup>+</sup>.

**Ethylcholest-5-en-3-hydroxy-7-one (12).** Amorphous powder; <sup>1</sup>H and <sup>13</sup>C NMR data (Fig. S48–S50) were found to be in agreement with previous study;<sup>25</sup> ESIMS *m/z* 429 [M + H]<sup>+</sup>.

**Coniferaldehyde (13).** Amorphous powder; <sup>1</sup>H and <sup>13</sup>C NMR data (Fig. S51–S53) were found to be in agreement with previous study;<sup>26</sup> ESIMS *m/z* 201 [M + Na]<sup>+</sup>.

**4-Hydroxy-3,5-dimethoxy-benzaldehyde (14).** Amorphous powder; <sup>1</sup>H and <sup>13</sup>C NMR data (Fig. S54–S56) were found to be in agreement with previous study;<sup>27</sup> ESIMS *m/z* 205 [M + Na]<sup>+</sup>.

### *In vitro* cytotoxicity assay

The *in vitro* cytotoxic effects of compounds **1–14** against human oral squamous cell carcinoma (SCC2095), human breast adenocarcinoma (MCF-7), human gastric adenocarcinoma (SCM-1), and fibroblasts were evaluated using MTT assays, following the method described in our previous study.<sup>28</sup>

Tamoxifen, etoposide, and paclitaxel were obtained from Sigma-Aldrich (USA).

## Author contributions

Thanh Hao Huynh: methodology, investigation, data curation, formal analysis, writing – original draft. Bo-Rong Peng: methodology, investigation, validation, writing – original draft. Chi-Jen Tai: methodology, investigation, data curation, formal analysis. Yu-Ting Hung: investigation, data curation. Yu-Chuan Su: investigation, data curation. Jing-Lan Hu: methodology, investigation, data curation. Jou-Hsuan Lee: investigation, data curation, Chang-Yih Duh: methodology, investigation, data curation, formal analysis. Jing-Ru Weng: conceptualization, resources, supervision, project administration, funding acquisition, writing – review & editing.

## Conflicts of interest

The authors declare that they have no known competing financial interests or personal relationships that could have appeared to influence the work reported in this paper.

## Data availability

Supplementary information: The data supporting this article have been included as part of the SI. ESIMS, HRESIMS, IR, 1D and 2D NMR spectra of compounds **1** and **2**; ESIMS and 1D NMR spectra of compounds **3–14**. See DOI: <https://doi.org/10.1039/d5ra03726c>.

## Acknowledgements

This study was supported by grants from National Science and Technology Council (grant no. NSTC 113-2320-B-110-005-MY3, NSTC 113-2320-B-110-007-MY3, and MOST 107-2313-B-110-003-MY3).

## Notes and references

- 1 F. Bray, M. Laversanne, H. Sung, J. Ferlay, R. L. Siegel, I. Soerjomataram and A. Jemal, *Ca-Cancer J. Clin.*, 2024, **74**, 229–263.
- 2 J. Ferlay, M. Colombet, I. Soerjomataram, D. M. Parkin, M. Piñeros, A. Znaor and F. Bray, *Int. J. Cancer*, 2021, **149**, 778–789.
- 3 S.-Y. Yin, W.-C. Wei, F.-Y. Jian and N.-S. Yang, *J. Evidence-Based Complementary Altern. Med.*, 2013, **2013**, 302426.
- 4 X.-F. He, X.-N. Wang, L.-S. Gan, S. Yin, L. Dong and J.-M. Yue, *Org. Lett.*, 2008, **10**, 4327–4330.
- 5 H. Liu, J. Heilmann, T. Rali and O. Sticher, *J. Nat. Prod.*, 2001, **64**, 159–163.
- 6 N. Bhardwaj, A. Sharma, N. Tripathi, B. Goel, G. Ravikanth, S. K. Guru and S. K. Jain, *Steroids*, 2023, **200**, 109315.
- 7 A. A. Naini, T. Mayanti and U. Supratman, *Arch. Pharm. Res.*, 2022, **45**, 63–89.



- 8 Y. Kashiwada, T. Fujioka, J. J. Chang, I. S. Chen, K. Mihashi and K. H. Lee, *J. Org. Chem.*, 1992, **57**, 6946–6953.
- 9 A. Singh, P. Chibber, P. Kolimi, T. A. Malik, N. Kapoor, A. Kumar, N. Kumar, S. G. Gandhi, S. Singh and S. T. Abdullah, *Int. Immunopharmacol.*, 2019, **69**, 34–49.
- 10 R. G. Naik, S. Kattige, S. Bhat, B. Alreja, N. De Souza and R. Rupp, *Tetrahedron*, 1988, **44**, 2081–2086.
- 11 V. Lakshmi, K. Pandey, A. Kapil, N. Singh, M. Samant and A. Dube, *Phytomedicine*, 2007, **14**, 36–42.
- 12 V. Lakshmi, K. Pandey and S. K. Agarwal, *Acta Ecol. Sin.*, 2009, **29**, 30–44.
- 13 K.-S. Hsu, *Plants of Lanyu*, Taiwan Department of Education, Taichung, 1982.
- 14 C.-E. Chang, *Flora of Taiwan*, 2nd edn, vol. 3, Epoch Publishing, Taipei, 1993.
- 15 S. Kurimoto, Y. Kashiwada, K.-H. Lee and Y. Takaishi, *Phytochemistry*, 2011, **72**, 2205–2211.
- 16 S. Kurimoto, Y. Kashiwada, S. L. Morris-Natschke, K.-H. Lee and Y. Takaishi, *Chem. Pharm. Bull.*, 2011, **59**, 1303–1306.
- 17 T. Fujioka, A. Sakurai, K. Mihashi, Y. Kashiwada, I.-S. Chen and K.-H. Lee, *Chem. Pharm. Bull.*, 1997, **45**, 68–74.
- 18 T. Fujioka, A. Sakurai, K. Mihashi, Y. Kashiwada, I.-S. Chen and K.-H. Lee, *Chem. Pharm. Bull.*, 1997, **45**, 202–206.
- 19 Y. Kashiwada, T. Fujioka, J.-J. Chang, I.-S. Chen, K. Mihashi and K.-H. Lee, *Bioorg. Med. Chem. Lett.*, 1992, **2**, 395–398.
- 20 H. Achenbach and D. Frey, *Phytochemistry*, 1992, **31**, 4263–4274.
- 21 D. T. T. Huong, T. T. T. Thuy, T. T. Hien, N. T. Tra, N. Q. Tien, I. Smirnova, O. Kazakova, E. Minnibaeva and G. Tolstikov, *Chem. Nat. Compd.*, 2013, **49**, 58–65.
- 22 O. Santana, M. Reina, B. M. Fraga, J. Sanz and A. González-Coloma, *Chem. Biodiversity*, 2012, **9**, 567–576.
- 23 N. Kovganko and Y. G. Chernov, *Chem. Nat. Compd.*, 1996, **32**, 183–186.
- 24 J.-H. Yang, Y.-F. Mei, R. Lu, Q. He, W.-W. Zhou and Y.-S. Wang, *Chem. Nat. Compd.*, 2020, **56**, 169–172.
- 25 A. Badreddine, A. Zarrouk, T. Nury, Y. El Kharrassi, B. Nasser, M. C. Malki, G. Lizard and M. Samadi, *Steroids*, 2015, **99**, 119–124.
- 26 T. T. San, Y.-H. Wang, D.-B. Hu, J. Yang, D.-D. Zhang, M.-Y. Xia, X.-F. Yang and Y.-P. Yang, *Bioorg. Med. Chem. Lett.*, 2021, **31**, 127682.
- 27 J.-J. Chen, C.-S. Yang, Y.-H. Chen, C.-Y. Chao, Y.-C. Chen and Y.-H. Kuo, *Molecules*, 2023, **28**, 2903.
- 28 L.-Y. Bai, J.-H. Su, C.-F. Chiu, W.-Y. Lin, J.-L. Hu, C.-H. Feng, C.-W. Shu and J.-R. Weng, *Mar. Drugs*, 2021, **19**, 244.
- 29 K. Jiang, L.-L. Chen, S.-F. Wang, Y. Wang, Y. Li and K. Gao, *J. Nat. Prod.*, 2015, **78**, 1037–1044.
- 30 M. Karplus, *J. Am. Chem. Soc.*, 1963, **85**, 2870–2871.
- 31 G. Breen, E. Ritchie, W. Sidwell and W. Taylor, *Aust. J. Chem.*, 1966, **19**, 455–481.
- 32 F. L. Anet, *J. Am. Chem. Soc.*, 1962, **84**, 747–752.
- 33 N. Sheppard and J. J. Turner, *Proc. R. Soc. London, Ser. A*, 1959, **252**, 506–519.
- 34 X. N. Wang, C. Q. Fan, S. Yin, L. P. Lin, J. Ding and J. M. Yue, *Helv. Chim. Acta*, 2008, **91**, 510–519.

